Two-wire guides and traps with vertical bias fields on atom chips

K. Brugger,[1] P. Krüger,[1,*] X. Luo,[1] S. Wildermuth,[1] H. Gimpel,[1] M. W. Klein,[1] S. Groth,[1] R. Folman,[1,†] I. Bar-Joseph,[2] and J. Schmiedmayer[1]

[1]*Physikalisches Institut, Universität Heidelberg, D-69120 Heidelberg, Germany*

[2]*Department of Condensed Matter Physics, Weizmann Institute of Science, Rehovot 76100, Israel*

(Received 17 July 2004; revised manuscript received 31 March 2005; published 10 August 2005)

We present atom chip traps and guides created by a combination of two current-carrying wires and a bias field pointing perpendicular to the chip surface. These elements can be arranged in any orientation on the chip surface. We study loading schemes for the traps and present a detailed study of the guiding of thermal atomic clouds in an omnidirectional matter waveguide along a 25-mm-long curved path at various atom-surface distances (35–450 μm). An extension of the scheme for the guiding of Bose-Einstein condensates is outlined. Such a concept enables utilizing the full two-dimensional surface of the chip.

DOI: 10.1103/PhysRevA.72.023607 PACS number(s): 03.75.Be, 39.90.+d

I. INTRODUCTION

The fast development of new tools for the precise control and manipulation of neutral atoms makes a great variety of novel experiments feasible. In particular, the adaption of microfabrication techniques in atom optics laboratories has led to the implementation of *atom chips* [1,2]. The patterned surfaces of these devices enable trapping and guiding of atoms with the high accuracy given by the fabrication process. Possible applications of atom chips are abundant; fundamental studies of degenerate quantum gases in low-dimensional potentials and mesoscopic physics in small atomic ensembles are two prominent examples. In the quest for implementations of quantum-information processing (QIP) with neutral atoms, atom chips are especially promising candidates.

The versatility of atom chips has been shown in a number of experiments. After the demonstration of simple magnetic trapping and guiding potentials [3–6], the production of Bose-Einstein condensates (BEC's) [7–10] and the integration of electrostatic fields on chips [11] have been important milestones on the way to a fully functional toolbox for the control of atomic matter waves. Issues currently under investigation include the integration of light elements for enhanced detection efficiency of (single) atoms [12] and the coherence properties of atoms in the chip potentials [13].

Here, we report on the implementation and experimental test of another key element for controlled manipulation of matter waves on atom chips: traps and guides with vertical bias fields. They have the advantage that the potential is independent of the orientation of the wires on the chip. In previous work such a geometry was used to demonstrate a guide based on a potential that is independent of the guiding direction [14]. Here, we present a detailed investigation of the guiding dynamics in this guide and elaborate on different loading schemes for this type of guide. Furthermore, traps created by vertical bias fields have been studied, allowing one to smoothly connect a trapping site to the demonstrated atom guide. Two-dimensional (2D) arrays of such individual trapping sites linked by the atom guide could be used for the implementation of quantum registers for QIP. In addition, the directional symmetry of this type of guide is crucial for guided matter wave interferometers that rely on spatially symmetric beam splitters—i.e., (wide-angle) Mach-Zehnder and Sagnac interferometers. Configurations in which the bias field is parallel to the chip surface suffer from an inherent symmetry breaking of any beam splitter, as different directions are exposed to effectively different bias fields.

II. THEORETICAL BACKGROUND: THE CONFINING POTENTIALS

The simplest form of a magnetic wire guide is the *side guide* [Fig. 1(a)] formed by superimposing the field of a current-carrying wire with a homogeneous external bias field parallel to the chip surface (horizontal) and perpendicular to the wire [1,3,4]. Atoms in a weak field seeking state are guided in a potential tube along a line parallel to the (straight) current-carrying wire.

The value of the potential minimum depends on the longitudinal component (along the guide) of the magnetic field. Changing the angle between the guiding wire and the bias field will vary the longitudinal field component and consequently the potential minimum of the guide. A changing value for the latter will constitute a trap or barrier for the guided atoms. For typical bias fields ($\sim$10 G) a change of angle of 100 μrad results in a barrier of 1 mG which significantly hinders guiding of a BEC.

Alternatively, if the bias field is orthogonal to the chip surface, the potential minimum is independent of the direction of the wire. But in this case the location of the minimum moves into the plane of the chip [Fig. 1(b)]. Guiding and trapping will now only be possible if either the wire is mounted on a ridge or a trough is etched into the chip surface so that the atoms can move freely without touching the surface.

Single-wire omnidirectional guiding above the plane of the atom chip therefore requires a horizontal bias field that

*Electronic mail: krueger@physi.uni-heidelberg.de

†Current address: Department of Physics, Ben Gurion University, Beer-Sheva 84105, Israel.

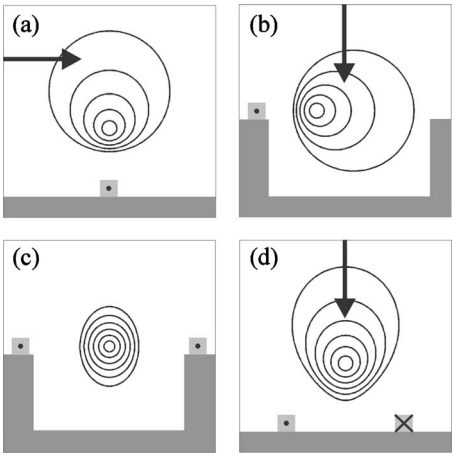

FIG. 1. The *upper* row presents the potential for a one-wire side guide generated by a single wire on the chip surface and an external bias field (a) parallel and (b) perpendicular to the atom chip. The *lower* row presents the field configuration for a two-wire guide with (c) parallel currents and no bias field and (d) counterpropagating currents and an external bias field perpendicular to the plane containing the wires.

follows with high accuracy the bending of the guide in order to maintain the perpendicular angle between the field and the guiding wire. This is obviously a complex task and in any case requires a locally produced bias field (e.g., by additional wires running in parallel to the guiding wire [15]). For the much simpler externally applied global bias fields, the field must undoubtedly be perpendicular to the chip surface.

In the following we will discuss some geometries for omnidirectional guiding. We will show how these schemes can be extended to guide BEC's using time orbiting potentials. Finally, the formation of 3D traps using bias fields which are perpendicular to the surface of the atom chip will be discussed. We will restrict ourselves to cases where a homogeneous bias field may be applied globally.

A. Two-wire guides

1. Counterpropagating currents

The two-wire guide based on parallel *counterpropagating* currents [Fig. 1(d)] requires a *vertical* bias field and hence enables omnidirectional guiding. Here, the field of the wires is compensated by a field pointing perpendicular to the wire plane. Now the two wires and therefore the atom guide can be bent in an arbitrary way in the plane perpendicular to the bias field, without the formation of any barrier or symmetry breaking.

Together with the currents, the strength of the bias field determines the height of the guide *above* the wire plane and the potential parameters [15]. Depending on the strength of the magnetic bias field B_b relative to the critical bias field

$$B_{crit} = \mu_0 I_w / \pi d \tag{1}$$

(where μ_0 is the vacuum permeability and d half the distance between the wires which carry currents of I_w each), we can distinguish three different cases as illustrated in Fig. 2.

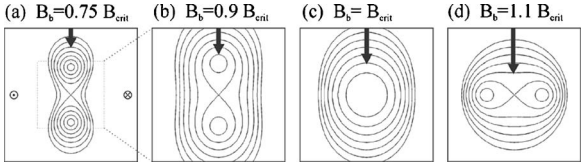

FIG. 2. Equipotential lines for the magnetic potentials in a two-wire guide with counterpropagating currents and bias fields orthogonal to the wire plane, with different field strengths. In (a) the position of the wires and the direction of the currents is shown. (a), (b) For $B_b < B_{crit}$ one finds two guides above each other, one above and one below the plane of the wires. These two combine at $B_b = B_{crit}$ (c) and then split up into two side guides in the plane of the wires for $B_b > B_{crit}$ (d).

For $B_b > B_{crit}$ each wire forms a side guide [Fig. 2(d)]. These guides are located in between the wires in the plane of the wires.

In the case $B_b = B_{\mathrm{crit}}$ the two side guides merge in the middle in between the two wires to a single guide in the plane of the wires (Fig. 2(c)).

In the regime $B_b < B_{\mathrm{crit}}$ one finds two minima above and below the wire plane [Figs. 2(a) and 2(b)] at a distance

$$r_0 = d\sqrt{\left(\frac{\mu_0}{\pi}\right)\frac{I_w}{dB_b} - 1}. \tag{2}$$

On the atom chip only the minimum above the chip surface is accessible. Close to the minimum the magnetic field is a two-dimensional quadrupole field with a gradient

$$\left.\frac{dB}{dr}\right|_{r_0} = \left(\frac{2\pi}{\mu_0}\right)\frac{B_b^2}{I_w}\frac{r_0}{d}. \tag{3}$$

For $B_b = \frac{1}{2}B_{\mathrm{crit}}$ the distance between the atom guide and the surface is half the distance between the wires ($r_0 = d$). In this case one obtains the largest potential depth and the gradient is the same as for the single-wire guide.

In a first experiment, a free-falling atomic cloud has been observed to be guided by a straight two-wire guide with counterpropagating currents [5].

2. Copropagating currents

One other possible two-wire guide is based on two parallel wires carrying *copropagating* currents [Fig. 1(c)]. The magnetic field formed by two parallel wires carrying copropagating currents vanishes along the central line between the wires and increases and changes direction like a two-dimensional quadrupole. Therefore no additional bias field is needed and the guide can be shaped simply by bending the wires.

Such wire guides with two copropagating currents have been realized, and it has been shown that atoms can be guided around moderate curves [6]. Cold atoms have even been stored in a complete loop. In these experiments a cloud has been observed to move around a number of full turns [16].

A drawback of these guides, however, lies in the fact that the rotational symmetry of the potential can only be main-

tained when no external bias field is added.[1] This implies that the *single* potential minimum will always be located in the center between the two wires—that is, in the plane of the wires—which limits the flexibility severely.

B. Time orbiting potential guide

Once a smooth omnidirectional guide is formed—e.g., by the two-wire counterpropagating current scheme—its minimum of zero magnetic field can lead to Majorana spin flips of the atoms to nontrapped states [17].

To avoid Majorana spin flips one can apply a magnetic field B_{ip} along the wires (IP field). This changes the form of the potential to harmonic with curvature

$$\left.\frac{d^2B}{dr^2}\right|_{r_0} = \left(\frac{2\pi}{\mu_0}\right)^2 \frac{B_b^4}{B_{ip} I_w^2} \frac{r_0^2}{d^2}, \tag{4}$$

whereby the zero magnetic field no longer exists. However, this may only be done by a (static) global external field if the guide is straight, in contradiction to the aim of omnidirectional guiding. For a multidirectional guide a locally varying field would have to be used or, alternatively, the IP field could be rotated as a (small) cloud moves along the guide.

Here, we suggest a more flexible solution that appears to be simple to implement experimentally. This solution is based on a periodical variation of the currents in the guiding wires themselves. A sinusoidal modulation of the currents according to

$$I(t) = I_0 + \sqrt{2} I_{\mathrm{mod}} \sin(\omega_{\mathrm{mod}} t + \phi) \tag{5}$$

in the two guiding wires with a relative phase difference of $\Delta\phi = \pi/2$ leads to a nearly circular motion of the quadrupole minimum of the guide (Fig. 3). As long as the modulation frequency ω_{mod} is slow with respect to the Larmor frequency ω_{Larmor} but fast with respect to the atomic oscillation frequency ω_{trap}, the atoms can be described as moving in a time orbiting potential (TOP). Such TOP's have successfully been used for the production of Bose-Einstein condensates [18]. The integrals for obtaining the average potential can generally only be solved numerically. In an ideal quadrupole field approximation the average field is given by elliptic functions whose Taylor expansion yields a parabolic leading term. Thus, the trap can be viewed as harmonic and the definition of a trap frequency $\omega_{\mathrm{trap}}/2\pi$ is meaningful. If the height h of the guide over the wire plane is equal to the half distance d between the wires, the characteristic frequencies of the trap simplify to

$$\omega_{\mathrm{Larmor}} = \frac{g_F \mu_B B}{\hbar} \frac{I_{\mathrm{mod}}}{I_0}, \tag{6}$$

and

$$\omega_{\mathrm{trap}} = \frac{2\pi}{\mu_0} \sqrt{\frac{g_F m_F \mu_B}{2M} \frac{B^3}{I_0 I_{\mathrm{mod}}}}, \tag{7}$$

with the vacuum permeability μ_0, the Bohr magneton μ_B, Landé factor g_F, and atomic mass M. The radius of the circle of vanishing field (circle of death) may be expressed in units of d or in units of the harmonic oscillator ground state size $a_0 = \sqrt{\hbar/M\omega_{\mathrm{trap}}}$:

$$r_0 = d\frac{I_{\mathrm{mod}}}{I_0} = a_0 \sqrt{\frac{m_F}{2} \frac{\omega_{\mathrm{Larmor}}}{\omega_{\mathrm{trap}}}}. \tag{8}$$

Thus, fulfilling the condition $\omega_{\mathrm{Larmor}} \gg \omega_{\mathrm{mod}} \gg \omega_{\mathrm{trap}}$—i.e., $\omega_{\mathrm{Larmor}}/\omega_{\mathrm{trap}} \gg 1$—will automatically ensure that the radius of the circle of death is much larger than the extension of a guided cloud in the ground state of the guide. For strongly interacting BEC clouds, the enlarged ground state may put a constraint on a minimal r_0 which would in turn automatically secure the above condition on the frequencies.

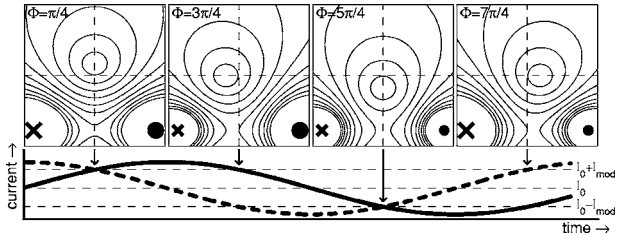

FIG. 3. Time sequence over one oscillation period of a time orbiting guiding potential. *Top*: the magnetic field of the guide is shown in a plane perpendicular to the two wires. The direction of the wire current is indicated by the dot and cross, and its magnitude corresponds to the size of the symbols. The dashed lines indicate the position of the minimum of the trap in the static case. *Bottom*: each of the counterpropagating currents (solid and dashed curves) in two parallel wires is sinusoidally modulated around the steady current I_0. A relative phase difference of $\Delta\phi = \pi/2$ results in a quadrupole field zero circling around the minimum of the static situation. With a proper choice of the modulation frequency, cold atoms are trapped in the time-averaged potential. While the position of the potential minimum remains unchanged with respect to the static case, the atoms never encounter a magnetic field zero and thus do not undergo Majorana spin flips.

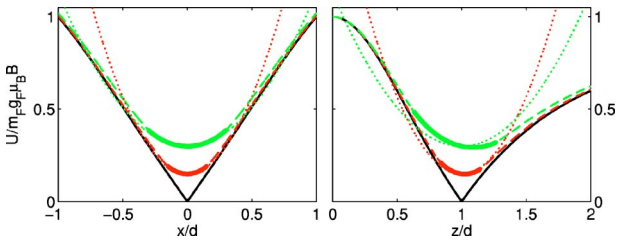

FIG. 4. (Color online) Numerical calculation of the TOP for the $d=h$ case for $I_{\mathrm{mod}}/I_0 = 15\%$ [red (online)/dark gray (print)] and 30% [green (online)/light gray (print)]. The potentials are plotted versus the position perpendicular to the wires with respect to the guide's minimum (left) and as a function of height over the wire plane (right). The length units are given in half wire separations d; the energy scale is given in units of the bias field B. Inside the circle of death, the potentials are depicted as thick solid lines, outside as dashed lines. For comparison, the harmonic approximation [Eqs. (7) and (9)] (dotted lines) and the static potential (black lines) are shown.

[1] Configurations with external bias field are discussed, e.g., in [1]

TABLE I. Realistic parameters for TOP two-wire guides on atom chips. The resulting potential characteristics are calculated for ^{87}Rb atoms in the $|F=2,m_F=2\rangle$ state.

d (μm)	B (G)	I_0 (mA)	I_{mod} (mA)	ω_{Larmor} (2π MHz)	ω_{trap} (2π kHz)	r_0 (μm)	U_{depth} (k_B μK)
1	40	20	3	4.2	150	0.15	110
1	40	20	5	7	110	0.25	180
1	40	20	8	11	90	0.4	290
10	20	100	4	0.6	20	0.4	15
10	20	100	10	1.4	13	1	37
10	20	100	40	5.6	6.4	4	150
50	20	500	10	0.3	5.7	1	7
50	20	500	50	1.4	2.5	5	37
50	20	500	200	5.6	1.3	20	150

The depth of the TOP is given by the average fields at r_0 and at the center of the guide:

$$B_{\mathrm{TOP}}(r_0) - B_{\mathrm{TOP}}(0) = \left(\frac{4}{\pi} - 1\right)\frac{I_{\mathrm{mod}}}{I_0}B \approx 0.27\frac{I_{\mathrm{mod}}}{I_0}B. \quad (9)$$

The potential tuning range is large; a few example configurations and the resulting guide parameters are listed in Table I.

These parameters are calculated according to the above formulas. The deviations from the used approximations grow as the ratio I_{mod}/I_0 is increased and as h/d deviates from unity. This can be observed in numerical potential calculations. The results of such calculations in the $h=d$ case are plotted for two different current modulation ratios (Fig. 4), and Fig. 5 shows the corrections for the circle of death.

Finally, adding local electric or magnetic field gradients (e.g., with alternating electrodes [11]), one may achieve dynamic confinement along the guide, thus turning it into an omnidirectional "conveyor belt."

C. Traps with vertical bias fields

The omnidirectional guides (created with the help of a vertical bias field) which we have presented may be utilized to connect two points on the chip, provided there are traps in these points which may be smoothly connected to the guides. Examples of such traps are the vertical bias field traps presented in this section.

Traps using vertical bias fields can be formed by adding "end caps" to the vertical guiding potentials as shown in Fig. 6(a). The two end cap wires separated by a distance $2D$ close the trap. Antiparallel currents in the end caps give a strong quadrupolelike confinement. Potentials of such a trap for $d=57.5$ μm, $D=180$ μm, and currents of 2 A are shown in Fig. 7. In atom chip experiments only the potential minimum above the chip surface is accessible. The end cap wires create an additional vertical field component which together with the two-wire guide by itself forms a trap even without external bias field. The field strength of the end cap wires in the center is given by $B_D=(\mu_0/\pi)I/D$. An additional vertical bias field $\mathbf{B}_b$ parallel to $\mathbf{B}_D$ will lower the trap towards the chip surface. If $\mathbf{B}_b$ reaches the new critical value

$$\tilde{B}_{crit} = B_{crit} - B_D = B_{crit}\left(1 - \frac{d}{D}\right), \quad (10)$$

the two traps merge in the plane of the chip ($B_{\mathrm{crit}}=(\mu_0/\pi)I/d$ is again the critical magnetic bias field for the two-wire guide as discussed above). Increasing the bias field further one finds two traps in the plane of the chip.

But even before $B_b=\tilde{B}_{crit}$ the traps can have leaks at the ends for hot atoms. These can be seen in Fig. 7 by the connections of the higher equipotential lines for larger bias fields.

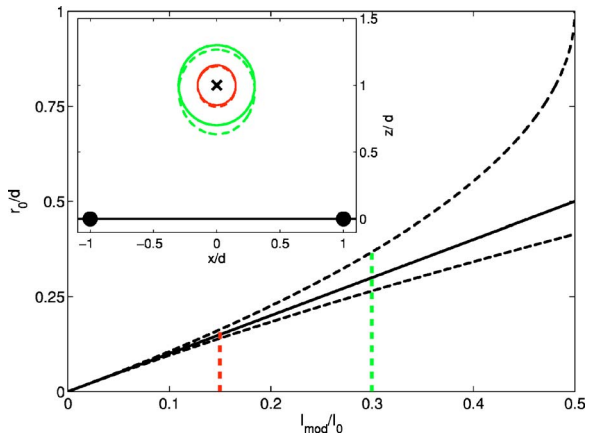

FIG. 5. (Color online) Deviations of the radius of the circle of death from Eq. (8) (solid line) in a full calculation. The dashed lines show the maximal and minimal distances of the field zero from the (average) potential minimum as functions of the current modulation I_{mod}/I_0. In the inset all positions of vanishing field are plotted (dashed lines) for the two cases $I_{\mathrm{mod}}/I_0=15\%$ [red (online)/dark gray (print)] and $I_{\mathrm{mod}}/I_0=30\%$ [green (online)/light gray (print)]. For comparison, the circles with the radius r_0 taken from Eq. (8) are shown (solid lines). The wire positions on the chip surface (black line) are marked as black solid circles; the length scales are given in units of the half wire separation d. The guiding potential minimum (both for the static and the TOP case) is marked as a black cross.

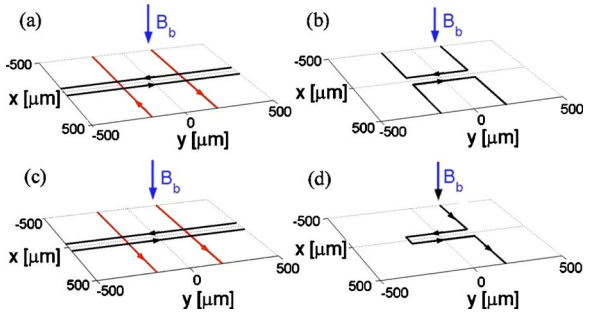

FIG. 6. (Color online) Four different wire configurations for traps with vertical bias fields. (a) A guide created by two parallel wires is closed to form a trap by two crossing wires with antiparallel currents. (b) A similar trap can be built by two U-shaped wires. (c) Similar to (a), but the currents through the two closing wires are parallel in this case, which avoids the magnetic field zero at the trap minimum. (d) This wire configuration leads to a similar trap as the configuration shown in (c), also avoiding zero magnetic field, but without the need of crossing wires.

Similar magnetic fields can be created by a double-U wire structure as shown in Fig. 6(b) which has been used in our experiments to trap thermal atoms. This geometry is easier to realize because no wire crossings are needed.

The vertical bias field traps described here have a magnetic field zero at their minima. This can be removed by applying a TOP as discussed above. Traps without zero magnetic field can also be achieved by the wire configurations shown in Figs. 6(c) and 6(d). The currents in the end caps are parallel in these cases leading to Ioffe-Pritchard-like magnetic fields. Potentials of a trap built by the wires shown in Fig. 6(c) and currents of 2 A can be seen in Fig. 8. The configuration of Fig. 6(d) leads to very similar potentials but has the advantage that no crossing wires have to be fabricated. In both cases the potentials are not symmetric.

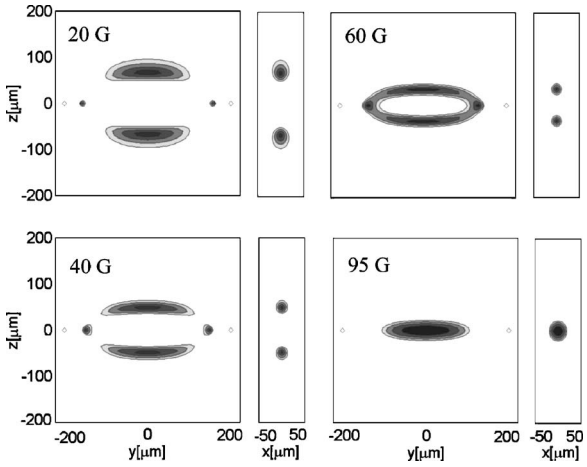

FIG. 7. Equipotential lines (separated by 300 μK for ^{7}Li in the $|2,2\rangle$ state) for the magnetic potentials in a two-wire vertical trap as shown in Fig. 6(a) and different bias fields strengths (see text for other parameters). The potential barrier towards the chip vanishes for a bias field of $B_b \geqslant \tilde{B}_{crit}$ (95 G for the given parameters).

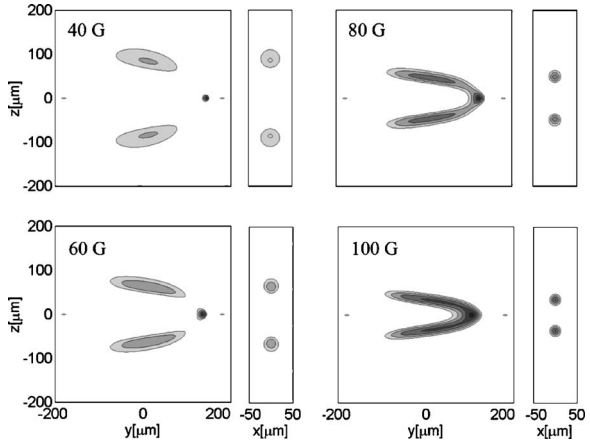

FIG. 8. Equipotential lines (separated by 300 μK for ^{7}Li in the $|2,2\rangle$ state) for the magnetic potentials in a two-wire vertical trap as shown in Fig. 6(c) and different bias field strengths (I_w=2 A).

III. EXPERIMENTAL SETUP

In the experiments described in this work, we set out to demonstrate the deterministic loading of traps and guides with vertical bias fields and the actual transport of atoms confined in such an omnidirectional two-wire guide with counterpropagating currents over an angle $>4\pi$.

The atom chips we have used for our experiments are made of a 5-μm gold layer placed on a 0.6-mm-thick Si substrate [19]. The chip wires are defined by boundaries of 10-μm-wide isolating gaps. This leaves the chip as a gold mirror (with 10-μm gaps), and it can be used to reflect the laser beams for the magneto-optical trap (MOT) during the cooling and collecting of atoms. For our experiments, we designed an atom chip with various double-U traps and a spiral-shaped two-wire guide (Fig. 9).

The starting point of our atom chip experiments is a reflection MOT [1,3,20] that contains a cloud of typically 10^8 cold ^{7}Li atoms located a few millimeters above the chip surface. Typically the pressure in the vacuum chamber is 10^{-10} mbar. The magnetic quadrupole field for the MOT is initially provided by external coils; after the loading it is replaced by the field of a U-shaped silver wire mounted directly underneath the chip ($\varnothing$=1 mm) which can carry currents of up to 24 A. By increasing the bias field, the MOT can be shifted towards the chip surface.

In the next step, the laser beams are switched off and the quadrupole field produced by the silver wire serves as a magnetic trap. The magnetic trap is then lowered further towards the surface of the chip by increasing the bias field until the atoms are close enough to be trapped by the chip fields. The details of this procedure are given in [4,21,22].

The atoms move within the magnetic potential for some time, and the resulting atomic distribution is studied using fluorescence light imaging. The images are taken by exposing the trapped atoms to a flash (100 μs) of near-resonant laser light. The linewidth of the imaging transition is 6 MHz, corresponding to a temperature of $\sim$300 μK. For most cases, the clouds had a smaller temperature, so that Zeeman shifts do not detune the transition significantly and the fluorescence

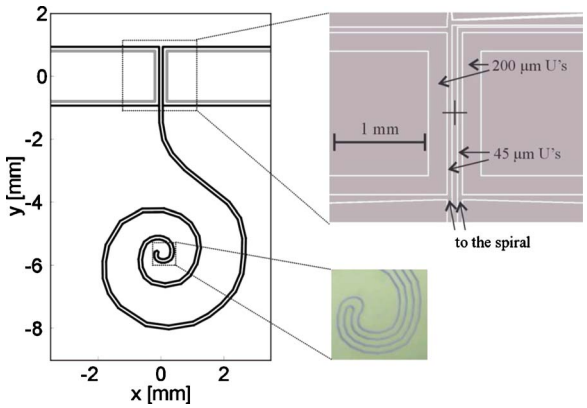

FIG. 9. (Color online) Chip design: *Left*: schematic drawing of the spiral-shaped wire. The black and gray lines indicate current-carrying wires; the white areas are grounded parts of the chip surface. *Top right*: the design of the double-U traps. The gold is shown in gray and the 10-μm gaps are white lines. The origin of the coordinate system used in the text is indicated by the cross. The two 45-μm-wide U wires are part of the spiral-shaped wire forming the omnidirectional guide. *Bottom right*: microscope image of a detail of the spiral-shaped wire. The 10-μm-wide gaps from which the gold has been removed to define the wires appear as dark lines.

signal can be assumed to be proportional to the atom number when all experimental parameters are kept constant. In order to avoid any disturbing reflections, the light enters the chamber from two directions parallel to the chip surface.

IV. EXPERIMENTAL RESULTS

A. Traps with vertical bias fields

1. Vertical double-U trap

The chip used in our experiment has two pairs of U-shaped wires which can form double-U traps. The wires have a cross section of 45×5 μm^2 and 200×5 μm^2, with a center-to-center separation between the pairs of 115 μm and 380 μm, respectively. The length of the central wire is 1.87 mm and 1.6 mm, and the resistance of the U pairs is 1.6 Ω and 0.7 Ω, respectively. Figure 9, top right, shows the details of the design.

2. Loading the vertical double-U trap

The loading procedure of the vertical traps requires, in addition to the usual ramping of the currents, the rotation of the bias field from horizontal to vertical. The currents in the wires and the magnitude and rotation of the bias field have to be adjusted in such a way that the potential minimum is transferred smoothly from one trap to the next.

We have investigated different loading mechanisms. Atoms can be transfered into the final vertical trap using the 45-μm-wide double-U structure as an intermediate step or can be directly loaded from the silver U wires underneath the chip (Fig. 10). Since both loading procedures result in the same atom number in the final vertical trap, we discuss the direct loading in this paper:

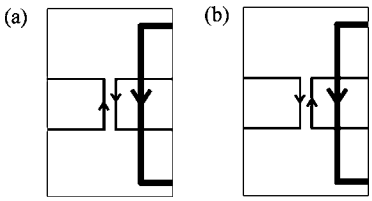

FIG. 10. Schematics of the currents in the silver U wire underneath the chip (thick line) and in the double-U wires from the vertical trap. In our setup the center of the silver U wire is 1200 μm below the chip surface. Two different loading geometries have been studied either using parallel currents (a) or antiparallel current (b) in the closest chip wire with respect to the silver U wire.

In this case two different loading geometries are possible: either using parallel currents or antiparallel currents in the closest chip wire with respect to the silver U wire. In the case of parallel loading there exists a closed trap during the whole process; i.e., the atoms can be loaded in an adiabatic way into the vertical trap, leading to a higher transfer efficiency. The procedure is shown in detail in Fig. 11.

The low-fluorescence signal of the final thermal atom cloud can be understood: (1) The atom cloud is compressed by about a factor of 10 in linear size which leads to a considerable increase in atom temperature (a calculated factor of

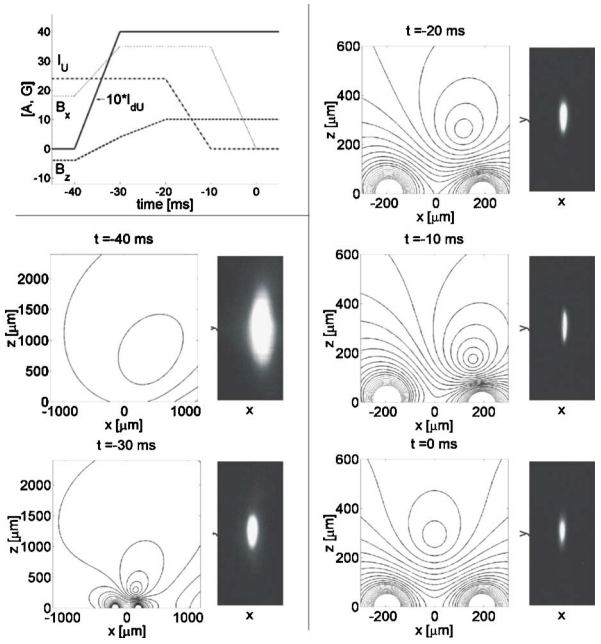

FIG. 11. (Color online) Parallel loading of the 200-μm vertical trap. *Top left*: time diagram of the currents and bias fields used in the loading process: I_U is the current through the silver U underneath the chip; B_x and B_z are the magnetic bias fields in the x and z directions, and I_{dU} is the current through the 200-μm-wide U wire ($\times10$). *Left*: xz cut through the calculated potential at $y=0$ with equipotential lines separated by $k_B\times400$ μK (definition of the x-y-z directions as in Fig. 9). *Right*: experimental fluorescence images of trapped atoms during the transfer in the xy plane (frame size 2150×4730 μm^2). The number of atoms is not proportional to the fluorescence intensity, since the trap parameters are changed during the transfer (see text).

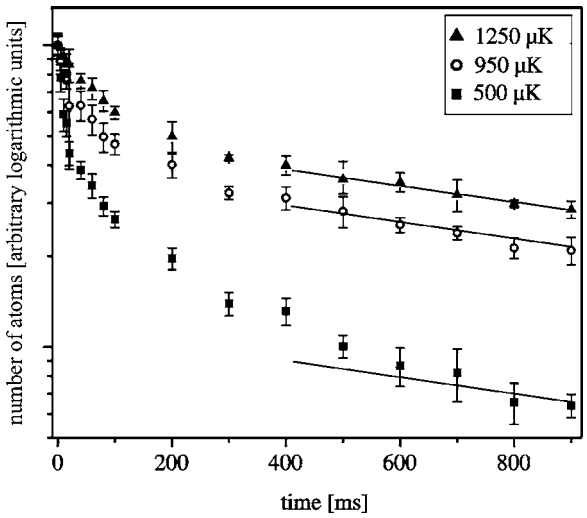

FIG. 12. Lifetime graphs of three-dimensional traps based on two counterpropagating currents in combination with a vertical bias field. Two different loss mechanisms can be distinguished in the time domain: An initial overexponentially fast process plays a role during the first ~100 ms; afterwards a slow exponential loss (time constant 1.6 s, solid lines) stemming from collisions with the background gas dominates. Both the rate and absolute magnitude of the fast loss depend on the depth of the trapping potential while the vacuum limited loss does not. The data were taken for traps with depths of $k_B \times 1250\ \mu$K, $950\ \mu$K, $500\ \mu$K (triangles, circles, squares, respectively). The error bars indicate the fluctuations in the fluorescence light. Note that during the first decay the atom number is underestimated due to the fact that the thermal energy of the atoms is higher than their natural linewidth.

about 5). Due to the limited trap depth, the compression leads to a reduced trapping volume. Hence the hot atoms are lost during the loading procedure. Much colder atoms or a BEC (which occupy the lowest-energy states of the trap only) will not leak from the trap. (2) Atoms in tight traps and high magnetic fields in general have smaller fluorescence due to optical pumping and increased detuning.

3. Trapping atoms in vertical double-U traps

The stability of the trapping in the vertical traps was investigated for various trapping parameters in the 45-μm-wide double-U trap. As a typical example we discuss a set of experiments with a current of 2 A and bias fields of 3 G, 10 G, and 15 G resulting in vertical traps at a distance of 220 μm, 160 μm, and 135 μm, from the chip surface and a trap depth of 500 μK, 950 μK, and 1250 μK, respectively.

Figure 12 shows the decrease of relative atom number with time for the three sets of trap parameters. One clearly sees an overexponential decay which lasts for a typical time of 100–400 ms. After this first decay, we observe an exponential decay with about 1.6 s lifetime. This latter decay is the same as observed with a side guide Z trap [1] under the same vacuum conditions. The initial fast decay can be attributed to the lower trap depth of the final compressed trap and is in good agreement with Monte Carlo (MC) calculations of the trapping process [22]. At longer times (up to ~500 ms) an additional decay occurs which the MC calculations do not take account of. We attribute this to a loss of hot atoms due to thermalization which is not included in the MC calculations. This loss and its time scale are clearly seen when looking at the width of the trapped cloud as shown in Fig. 13. In the region with stable trap width (stable temperature, no evaporation loss) the 1.6 s of the vacuum-limited lifetime is obtained. In this time domain the atom number is proportional to the fluorescence signal, whereas during the first decay the atom number is underestimated due to the fact that the thermal energy of the atoms is higher than their natural linewidth.

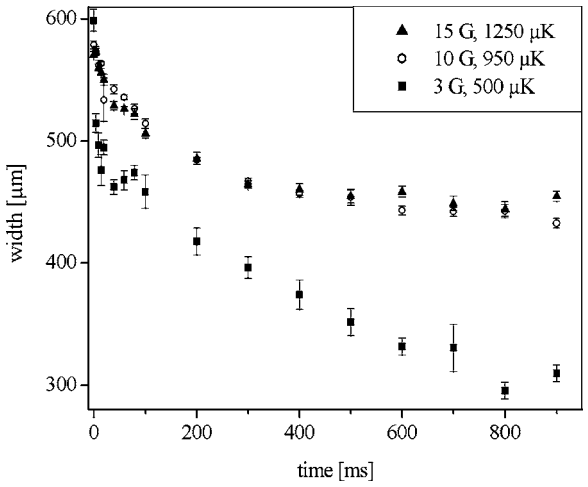

FIG. 13. Width of the longitudinal Gaussian fluorescence light distribution from a trapped atomic cloud. Decreasing width indicates loss of hot atoms. See text for explanations.

B. Two-wire spiral guide

1. Spiral guide

The two wires of the spiral guide (width $\times$ height $= 45 \times 5\ \mu m^2$, center-to-center spacing $2d = 115\ \mu$m) are connected at the inner end of the spiral (see Fig. 9). This automatically leads to a counterpropagating current flow. During the experiments we push a current of up to 1 A through the spiral wire (the total length of the spiral wire is 50 mm and it has a resistance of 8 Ω). The magnetic guiding potential of the spiral forms a tube for the atoms to move in (Fig. 14). The spiral shape was chosen in order to demonstrate the full flexibility of the guide by incorporating more than two full rotations with curve radii ranging from 200 μm to 3 mm along the 25-mm-long guiding path.

The potential depth of the guide is similar to the double-U trap with identical currents and bias fields. The longitudinal potential gradient (of the trap minimum magnetic field) at the beginning of the guide (as shown in the insert of Fig. 14) pushes the atoms from the trap region into the guide. This can be enhanced by additional currents through chip wires parallel to the leads (orthogonal to the initial direction of the guide). At the inner end of the spiral, the connection between the two wires creates an end cap where the atoms are reflected.

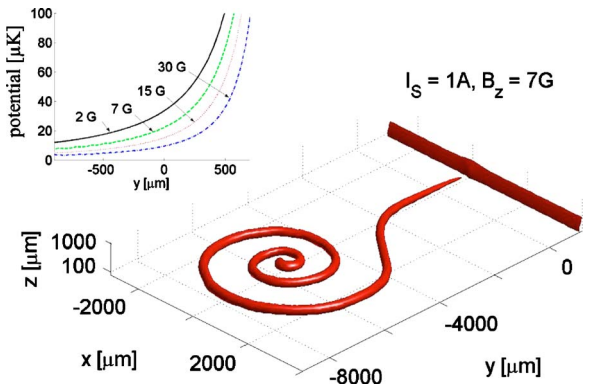

FIG. 14. (Color online) 400-μK equipotential surface of the spiral atom guide with a current of 1 A and a vertical bias field of 7 G. The inset shows the potential minimum for different magnetic bias fields (2 G, 7 G, 15 G, and 30 G) at the beginning of the guide. The longitudinal magnetic gradient pushes the atoms into the guide.

2. Loading the spiral guide

In our experiment we load the spiral guide directly from the silver U-trap.[2] In order to transfer the atoms from the silver U-wire trap—i.e., a trap based on a single wire and a horizontal bias field—to the spiral-shaped two-wire guide, we ramp down the current of the single wire after ramping up the counterpropagating currents in the two parallel wires of the guide. The changes in the currents and magnetic bias fields for the loading procedure are shown in Fig. 15.

The first part of the loading (until $t=-10$ ms, before the bias field is rotated) is similar to the double-U trap loading presented earlier. The atoms are trapped between the 90° bend of the wires at the beginning of the guide (at $y=900$ μm in Fig. 9) and the first bend in the two-wire guide (at $y=-2500$ μm). At this initial phase the two-wire guide actually acts as a single-wire side guide (with a small perturbation from the second wire). As the rotation of the bias field progresses, the spiral guide opens up continuously as the potential barrier caused by the bend in the guide gets smaller for a more vertical orientation of the bias field. Atoms with $E \geqslant k_B \times 450$ μK can pass the barrier already 4 ms before the end of the field rotation (at $t=-4$ ms), atoms with $E \geqslant k_B \times 250$ μK can pass the barrier 2 ms later (at $t=-2$ ms). Typical potentials before the rotation ($t=-10$ ms) of the bias field and close to the end of the loading procedure ($t=-4$ ms) are shown in Fig. 15.

In Fig. 15 we also present fluorescence images of the last 10 ms of the loading procedure. Atoms leak into the spiral guide (depending on their energy) even before the complete rotation of the bias field.

3. Guiding atoms in the spiral guide

Figure 16 shows a time sequence of the fluorescence signal of the atoms in the guide. Guiding of atoms was possible

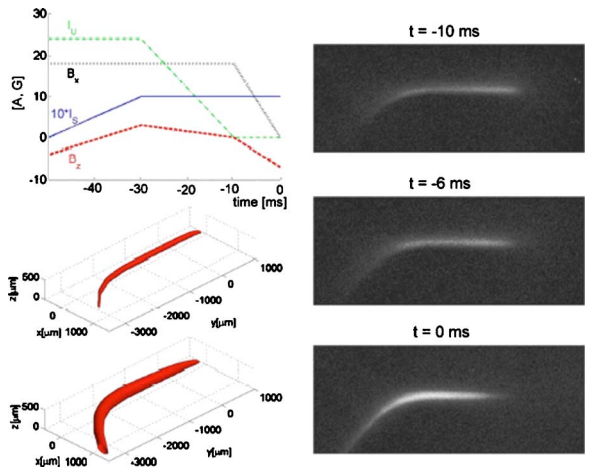

FIG. 15. (Color online) Loading of the spiral. *Top left*: time diagram of the variation in the currents and bias fields during the loading of the spiral guide. I_U is the current through the silver U underneath the chip, B_x and B_z are the magnetic bias fields in the x and z direction, and I_S is the current through the 45-μm-wide spiral wire ($\times 10$). *Middle left*: equipotential surface at 900 μK for the trap with 18 G horizontal bias field ($t=-10$ ms). *Bottom left*: equipotential surface at 500 μK during the rotation of the bias field at $t=-4$ ms (horizontal field 7.2 G, vertical field 4.2 G). The opening of the guide for atoms with $E>500$ μK is evident. *Right*: atomic fluorescence pictures during the loading process for different times from $t=-10$ ms until $t=0$ ms (frame size 2580 μm $\times$ 6450 μm in the xy plane). The fluorescence signal represents the distribution of the atoms during the loading of the guide. The number of atoms is not proportional to the fluorescence intensity, since the trap parameters are changed during the transfer (see text).

over a wide range of parameters. By varying the bias field strength B from 1 G to 50 G at a constant current of 1 A through both (connected) wires, the height of the potential tube above the surface was scanned from 450 μm to 35 μm. The corresponding gradients ranged from 40 G/cm to 8 kG/cm for atoms in the $|F=2,m_F=2\rangle$ state.

To investigate the time evolution of the atoms in the spiral we divided the fluorescence pictures into 215×215 μm^2 large pixels and measured the relative atom density in each pixel from the fluorescence intensity. Adding all pictures one finds the clear form of the spiral. From these one can select the pixels which define the trajectory of the spiral. To investigate the atom motion along the spiral guide we selected the pixels of the spiral and an additional row on both sides to sum up the fluorescence signal.

The images and density profiles in Fig. 16 show that the atom cloud not only expands according to its temperature,[3] but also moves as a whole along the guide. This center-of-mass motion is induced by the longitudinal field gradient, mentioned earlier, produced by the current in the two leads from the beginning of the spiral wires to the connecting pads on the edge of the chip. By running a parallel current through another wire on the chip, we could even enhance this "pushing" effect.

[2]It can also be loaded directly from the vertical trap by simply disconnecting the current in the leads on one side of the trap. Thus the barrier between the vertical trap and the vertical guide disappears.

[3]The clouds exhibit an anisotropic temperature profile (450 μK in the transverse, 50 μK in the longitudinal direction) due to a transverse compression during the loading without fast rethermalization.

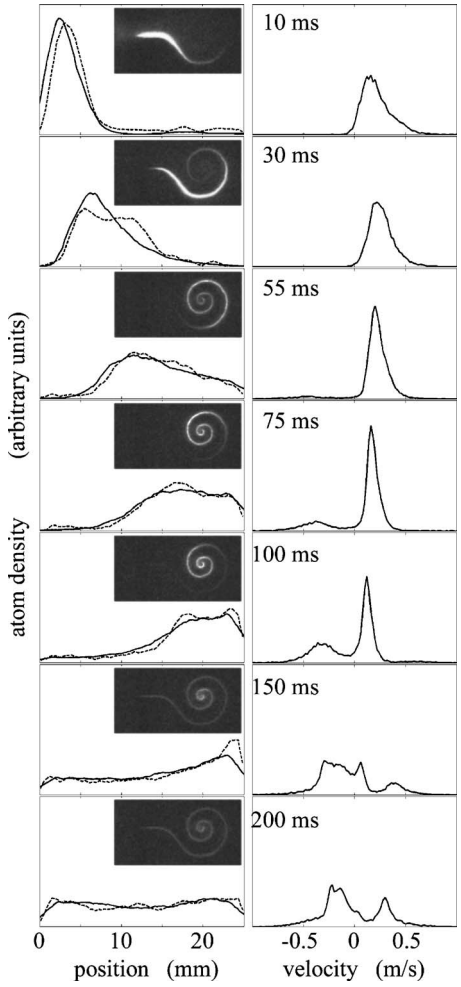

FIG. 16. *Left*: the one-dimensional atomic density profiles (solid curves) along the spiral-shaped guide are shown for different guiding times. A Monte Carlo simulation (dashed curves) is in good agreement with the observed propagation dynamics. The insets show corresponding fluorescence images of the atomic cloud. *Right*: velocity distributions of the atomic sample obtained by the same Monte Carlo simulation show a reflection of the propagating atoms at a potential barrier at the end of the guide (center of spiral). This reflection can be clearly seen in the fluorescence images of the atomic cloud (see insets).

For a quantitative understanding of the density profiles, we performed Monte Carlo simulations of classical trajectories of particles in the guide. The results are depicted in Fig. 16 and show good agreement with the experiment. In particular, the reflections that occur when atoms reach the inner end of the guide are reproduced. The effect of the reflection becomes most apparent in the plots of the velocity distributions extracted from the MC calculations (insets). The velocity classes for forward and backward motion in the guide are clearly separated.

Direct lifetime measurements in the guide were only carried out for guiding times of up to ~200 ms.[4] These measurements were then compared to the lifetime measurements performed in the vertical traps described earlier (based on counterpropagating currents through two parallel wires). The results are presented in Fig. 17. Because of the nearly identical behavior of the experimental lifetime plots for the trap and guide, we expect a similar comparison also on the longer time scales where only trap data are available.

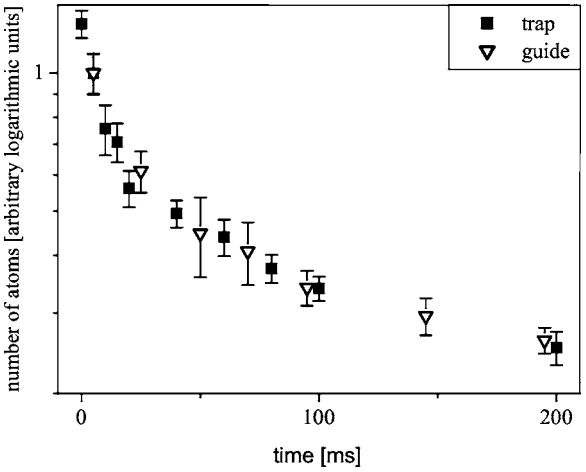

FIG. 17. Lifetime graphs showing a comparison between the lifetime of a three-dimensional trap (squares) and the guide (triangles) of approximately equal potential depth of $k_B \times 500\ \mu$K.

Finally, we note that the initial fast decays observed for both the trap and guide are not expected to pose a problem for much colder atoms or even a BEC, as the barrier heights relative to the sample temperature will be much higher.

V. CONCLUSION

To conclude, we have demonstrated the controlled loading and guiding of atoms in orientation-independent trapping and guiding potentials on an atom chip. The flexibility of an omnidirectional guide was proven by operating it over a wide parameter range. Monte Carlo simulations reproduce the measured time-dependent atomic density profiles, and hence the guiding dynamics are well understood and may be utilized for the design of more elaborate schemes.

To avoid Majorana spin flips for single-mode propagation, we have discussed a scheme involving time-dependent currents to modify the guide so as to circumvent its magnetic zero minimum.

Future applications range from the loading of two-dimensional trap arrays to the realization of circular or wide-angle matter wave interferometers [23].

ACKNOWLEDGMENTS

This work was supported by the European Union, Contract Nos. IST-2001-38863 (ACQP), HPRI-CT-1999-00114 (LSF), and HPRN-CT 2002-00304 (FASTNet) and the Deutsche Forschungsgemeinschaft, Schwerpunktprogramm "Quanteninformationsverarbeitung."

[4]Ohmic heating in the long guiding wires did not allow longer guiding times without risking damage to the wires.

[1] R. Folman, P. Krüger, J. Schmiedmayer, J. Denschlag, and C. Henkel, Adv. At., Mol., Opt. Phys. **48**, 263 (2002).
[2] J. Reichel, Appl. Phys. B: Lasers Opt. **74**, 469 (2002).
[3] J. Reichel, W. Hänsel, and T. W. Hänsch, Phys. Rev. Lett. **83**, 3398 (1999).
[4] R. Folman, P. Krüger, D. Cassettari, B. Hessmo, T. Maier, and J. Schmiedmayer, Phys. Rev. Lett. **84**, 4749 (2000).
[5] N. H. Dekker, C. S. Lee, V. Lorent, J. H. Thywissen, S. P. Smith, M. Drndić, R. M. Westervelt, and M. Prentiss, Phys. Rev. Lett. **84**, 1124 (2000).
[6] D. Müller, D. Z. Anderson, R. J. Grow, P. D. D. Schwindt, and E. A. Cornell, Phys. Rev. Lett. **83**, 5194 (1999).
[7] H. Ott, J. Fortagh, G. Schlotterbeck, A. Grossmann, and C. Zimmermann, Phys. Rev. Lett. **87**, 230401 (2001).
[8] W. Hänsel, P. Hommelhoff, T. W. Hänsch, and J. Reichel, Nature (London) **413**, 498 (2001).
[9] A. E. Leanhardt, A. P. Chikkatur, D. Kielpinski, Y. Shin, T. L. Gustavson, W. Ketterle, and D. E. Pritchard, Phys. Rev. Lett. **89**, 040401 (2002).
[10] S. Schneider, A. Kasper, C. vom Hagen, M. Bartenstein, B. Engeser, T. Schumm, I. Bar-Joseph, R. Folman, L. Feenstra, and J. Schmiedmayer, Phys. Rev. A **67**, 023612 (2003).
[11] P. Krüger, X. Luo, M. W. Klein, K. Brugger, A. Haase, S. Wildermuth, S. Groth, I. Bar-Joseph, R. Folman, and J. Schmiedmayer, Phys. Rev. Lett. **91**, 233201 (2003).
[12] P. Horak, B. G. Klappauf, A. Haase, R. Folman, J. Schmiedmayer, P. Domokos, and E. A. Hinds, Phys. Rev. A **67**, 043806 (2003).
[13] C. Henkel, P. Krüger, R. Folman, and J. Schmiedmayer, Appl. Phys. B: Lasers Opt. **76**, 173 (2003).
[14] X. Luo, P. Krüger, K. Brugger, S. Wildermuth, H. Gimpel, M. W. Klein, S. Groth, R. Folman, I. Bar-Joseph, and J. Schmiedmayer, Opt. Lett. **29**, 2145 (2004).
[15] J. H. Thywissen, M. Olshanii, G. Zabow, M. Drndic, K. Johnson, R. Westervelt, and M. Prentiss, Eur. Phys. J. D **7**, 361 (1999).
[16] J. A. Sauer, M. D. Barrett, and M. S. Chapman, Phys. Rev. Lett. **87**, 270401 (2001).
[17] C. V. Sukumar and D. M. Brink, Phys. Rev. A **56**, 2451 (1997).
[18] W. Petrich, M. H. Anderson, J. R. Ensher, and E. A. Cornell, Phys. Rev. Lett. **74**, 3352 (1995).
[19] S. Groth, P. Krüger, S. Wildermuth, R. Folman, T. Fernholz, D. Mahalu, I. Bar-Joseph, and J. Schmiedmayer, Appl. Phys. Lett. **85**, 2980 (2004).
[20] K. I. Lee, J. A. Kim, H. R. Noh, and W. Jhe, Opt. Lett. **21**, 1177 (1996).
[21] D. Cassettari, A. Chenet, R. Folman, A. Haase, B. Hessmo, P. Krüger, T. Maier, S. Schneider, T. Calarco, and J. Schmiedmayer, Appl. Phys. B: Lasers Opt. **70**, 721 (2000).
[22] K. Brugger, Ph.D. thesis, University of Heidelberg, 2004.
[23] E. Andersson, T. Calarco, R. Folman, M. Andersson, B. Hessmo, and J. Schmiedmayer, Phys. Rev. Lett. **88**, 100401 (2002).